

STATUS OF LISA INJECTOR

C. Biscari, A. Aragona, R. Boni, M. Castellano, V. Chimenti, A. Gallo, S. Kulinski*,
C. Sanelli, B. Spataro, F. Tazzioli, F. Tian^o and M. Vescovi

INFN, Laboratori Nazionali di Frascati, C.P.13, 00044 Frascati, Italy

**On leave of absence from Institute for Nuclear Studies, Swierk, Poland*

^oVisitor from I.H.E.P., P.O. BOX 918, Beijing, P.R.China

Abstract

The injector of the LNF project LISA (Linear Superconducting Accelerator) is a room temperature system, consisting of a transport line for the beam at 100 keV, of a capture section (a graded- β 2.5 GHz structure) which accelerates the beam to 1.1 MeV, and of an isochronous and achromatic transport line which injects the beam into the SC-Linac after a π -bending. The status of the project is presented.

Introduction

The superconducting (SC) electron linac LISA¹, in construction at Frascati INFN Laboratories, is a test-bench machine aimed at studying the larger SC linacs for colliders or CW machines for nuclear physics and at implementing a high efficiency FEL in the infrared wavelength region. In addition to the acquisition of the general techniques related to superconducting acceleration, LISA will allow to study such interesting topics as low emittance electron guns, beam recirculation and beam break-up that are fundamental in such machines.

In the first step of the project the beam parameters are mainly defined by the FEL application, which will require a 25 MeV beam and 5 A peak current. The bunch compression required to obtain this peak current from the 2 mA average current is performed in the injection system.

The injector² consists of the following major parts:

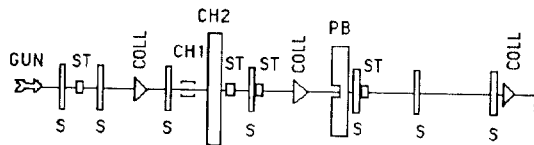
- 100 keV thermoionic gun.
- Double chopping system..
- 500 MHz prebuncher.
- 1 MeV, 2.5 GHz capture section.
- Achromatic and isochronous transport line between the capture section and the SC Linac.

The other elements of the injector are: solenoidal focusing lenses, steering coils, collimators, current monitors, fluorescent screens. All RF elements in the injector have been constructed and successfully tested. Their detailed description is presented in this conference³.

The injector will be installed starting from next autumn.

Injector Description

The block diagram of the 100 keV part of the injector is shown in Fig. 1.



S - Solenoidal lenses; ST - Steerings; COLL - Collimator;
CH1 - Chopper 1 (50MHz); CH2 - Chopper 2 (500MHz);
PB - Prebuncher (500MHz).

Fig.1 - Sketch of the injector line at 100keV.

The gun is a Pierce-geometry thermoionic triode which delivers a 1 ms macropulses beam at a repetition rate of 10Hz. It is presently under test⁴.

The design parameters are: current $I > 200$ mA, normalized emittance $\epsilon_n < 10^{-5}$ m rad, energy $W = 100$ keV, energy dispersion $\Delta W/W = 10^{-3}$.

A double chopping system has been chosen in order to operate with lower average current without diminishing the peak current, relaxing so the shielding requirements. The first chopper CH1 operates at the subharmonic frequency $f_1 = 50$ MHz and consists of a pair of deflecting electrodes. It selects 10% of the total current so that the beam afterwards is composed of a succession of micropulses at the frequency of 50 MHz. The second chopper CH2 is a RF rectangular copper cavity oscillating at $f = 500$ MHz in the deflecting TM₂₁₀ mode. It selects a phase spread $\Delta\Phi_{ch}$ ranging between 36° and 60° over the wavelength according to the accelerated percentage of the total current. Both choppers act deflecting vertically the beam; a pair of steerings corrects this deflection so that only the selected $\sim 1\%$ of the current passes through a collimator whose walls absorb the $\sim 99\%$ of the beam power.

The prebuncher is a klystron type microwave cavity oscillating in TM₀₁₀ mode at the same frequency of the superconducting cavities, followed by the corresponding drift ($D=1.44$ m). The gap length is one tenth of the wavelength; the voltage is of the order of 20 kV.

The capture section⁵ is a normal conducting S-Band, standing wave, biperiodic $\pi/2$ β -graded accelerator, working at the fifth harmonic of the basic frequency, $f_{CS} = 2500$ MHz. It prepares the injection of the electron bunches into the SC Linac with sufficiently large $\beta \approx 0.94$, small phase bunch length $\Delta\phi \approx 1^\circ - 2^\circ$ (@500MHz), and small energy dispersion $\Delta W/W \approx 1-2\%$. An axial magnetic field produced by superimposed solenoids counterbalances the radial defocusing forces due to either the space charge or to the radial component of the accelerating field. The main parameters of the section together with the power tests are described in Ref. 5.

The transport line between the capture section and the SC linac is achromatic to avoid dispersion in the horizontal phase plane and isochronous to avoid bunch lengthening. Since electrons are not fully relativistic at the injection energy, the spread in arrival time due to the energy spread has been taken into account and properly compensated with the trajectory length dependence on the dispersion function. The bending is obtained with three dipoles ($45^\circ, 90^\circ, 45^\circ$) and two symmetric quadrupole doublets which adjust the dispersion function η to the isochronism condition which corresponds to:

$$\eta = \frac{L}{\sqrt{2}\gamma} - 2\sqrt{2}\rho \left(\frac{\pi}{4} - \frac{\sqrt{2}}{2} \right)$$

at the midpoint of the central dipole (L is the total line length, ρ the bending radius). Two triplets in front and after the arc take care of the matching between the linacs and the arc itself.

In the matching line between the capture section and the arc, a pulsed magnet deviates the beam to the spectrometer; the pulse timing is such that a single macropulse can be extracted, or the whole beam derived to the spectrometer arm. The spectrometer consists of two 60° sector bending magnets and two quadrupoles. The beam dimensions are analyzed on a fluorescent screen.

A bunch length measurement⁶ is foreseen exploiting the spectrometer line: a vertically deflecting 2.5 GHz cavity, positioned before the pulsed magnet, gives an angular kick to the electrons depending on their position along the bunch, causing a vertical widening of the beam spot on the screen proportional to the bunch length.

To increase the sensitivity of the measurement a different set of quadrupole gradients will be used in this configuration which will give the optimum vertical phase advance between the cavity and the screen, so that while the energy measurement will be on-line this last diagnostic tool will be used off-line.

All the magnets have been designed by means of the 3-D code Magnus; they are constructed with full Armco iron, except the two spectrometer laminated dipoles. The full iron magnets are home-made while the two laminated are built by a French firm. The nominal characteristics of the magnetic elements are listed in table I and the layout of the transport line is plotted in fig. 2.

Table I - 1.1 MeV Transport Line Element Characteristics.

Element type	Length (cm)	Gradient (gauss/cm)	Bending angle (degrees)
QUAD	10.0	-18.5000	
QUAD	10.0	17.0700	
QUAD	10.0	-9.4570	
BEND	20.02765	1.1747	45.
QUAD	10.0	13.2754	
QUAD	10.0	-5.7083	
BEND	40.0553	1.1747	90.
QUAD	10.0	-5.7083	
QUAD	10.00	13.2754	
BEND	20.02765	1.1743	45.
QUAD	10.0	-10.7400	
QUAD	10.0	15.5000	
QUAD	10.0	-8.7500	

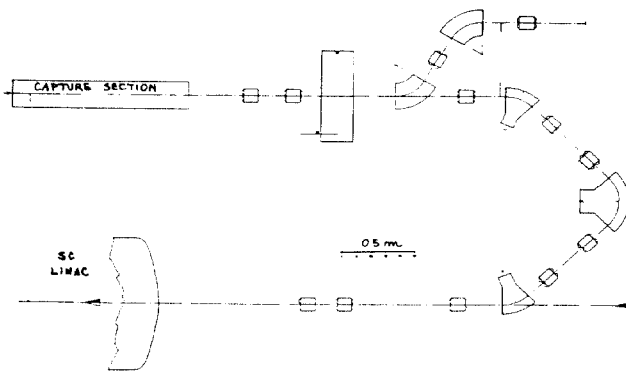


Fig. 2 - Layout of the transport line capture section - SC Linac.

Particle dynamics

Tracking of particles along the injector has been carried out with a modified version of the program PARMELA⁷ simulating different currents, in order to determine the acceptance of the system in different working conditions.

The extremely high beam quality required asks for a careful adjustment of all the components of the line from the very beginning. In fact space charge problems influence the bunch transverse dimensions and the longitudinal phase space all along the transport.

The nominal average current of 2 mA in the Linac can be obtained using an extracted beam from the gun of 200 mA and a chopping angle of CH2, $\Delta\phi_{ch} = 36^\circ$, or otherwise it is possible to decrease the initial current and to increase correspondingly $\Delta\phi_{ch}$. In fact the longitudinal space charge prevents the squeezing of the bunch to very short lengths at the input of the capture section. If the bunch length after the chopper system is longer the space charge effects are weaker for the same bunch charge; furthermore decreasing the beam current intensity between the gun and the choppers the emittance growth due to transverse space charge can be avoided. So $I_{gun} = 120$ mA and $\Delta\phi_{ch} = 60^\circ$ have been chosen.

The increase of the beam emittance at low energies can be further reduced if the bunch length is not led to its possible minimum at the input of the capture section keeping the current density below critical values. The high peak current at higher energies can be obtained using the appropriate phase in the capture section, so that in the first cells of the section the beam is still under the bunching process.

The longitudinal magnetic field produced by the solenoid around the section has been measured for different values of the current in the windings; the analytical expression obtained with a polynomial fit of the measured values has been introduced in the program PARMELA and used for particle tracking⁵.

At the exit of the capture section the beam has circular symmetry and is highly focalized by the magnetic field of the capture section solenoid.

If the beam size inside a quadrupole is above a certain value (in our case, with $\epsilon_{x,y} = 5.6 \times 10^{-6}$ m rad, $e_{lim} \sim 0.9$ cm) the quadrupole field produces filamentation in the transverse phase space yielding to increase of the effective emittance value: the focusing kick given by the quadrupole is not linear with the distance from the axis, but distorted. This effect of course is significant only at energies up to the order of few MeVs and at low emittances. As the horizontal emittance conservation is more critical than the vertical one because of the presence of horizontal dispersion along the line, in the optical functions design special care has been put in keeping lower the horizontal betatron function inside the quadrupoles.

The achromaticity condition on the horizontal plane is satisfied only if the particle trajectories and their energies are not perturbed inside the dispersive region, so that the correlation is maintained between the particle energy and the displacement of the particle trajectory from the nominal trajectory. The space charge breaks this correlation, resulting in an increase of the horizontal emittance of about 20% along the dispersive zone. An increase of about 10% on the emittance occurs also for the direct action of the space charge forces while another 10% is due to the filamentation above described. The final vertical emittance results almost equal to the horizontal one.

Analysis of the dipole fringing field on the particle trajectories has been carried out and the corresponding correction of the nominal trajectory has been calculated, resulting in a parallel displacement of 1. mm⁸.

The beam emittances along the injector are plotted in fig. 3. The bump of the horizontal emittance corresponds to the dispersive zone, because the momentum spread contribution to the beam size is included in the computation of the emittance.

The envelopes are plotted in fig. 4.

The bunch length is plotted in fig. 5, together with the length occupied by the 68% of the total current to have a comparison with the usual gaussian distribution.

Table II gives the beam parameters in the principal points of the line ($\epsilon_{x,y}$ are the transverse envelopes, l_b the bunch length).

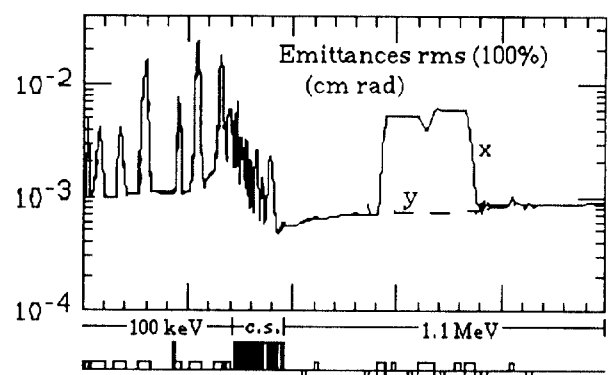


Fig. 3 - Beam emittances from gun to SC-Linac entrance.

Table II - Beam parameters along the injector.

Beam Parameters	Gun output	Capture Section Input	Capture Section Output	SC Linac Input
α_x	0.0	-6.0	0.66	-3.8
β_x (m)	0.025	0.5	0.24	4.4
ϵ_x (mm mrad)	10.0	18.0	5.6	9.2
e_x (mm)	0.5	3.1	1.2	0.6
α_y	0.0	-6.0	0.66	-0.6
β_y (m)	0.025	0.5	0.24	0.7
ϵ_y (mm mrad)	10.0	18.0	5.6	8.4
e_y (mm)	0.5	3.1	1.2	0.3
E_0 (MeV)	0.10	0.098	1.17	1.17
$\Delta E/E$ (%)	0.01	± 4.5	± 1.5	± 3.0
l_b (100%) (mm)	continuous	7.0	3.1	3.8
l_b (68%) (mm)	continuous	4.5	1.2	1.8
I_{av} (mA)	120.	2.	2.	2.
I_p (A)	0.12	<1.	6.4	4.3

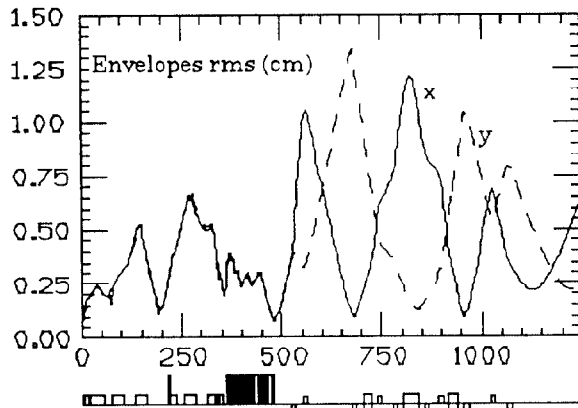


Fig. 4 - Beam transverse envelopes from gun to SC-Linac entrance.

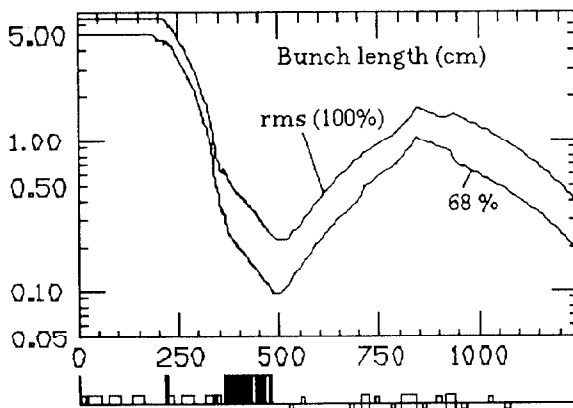


Fig. 5 - Bunch length from gun to SC-Linac entrance.

Tolerances

Tolerances of the line up to the capture section have been checked with PARMELA simulations: 10% errors in the field intensities of magnetic lenses do not change appreciably the line transmission, while 1% precision in the field of the capture section solenoid is needed. The prebuncher voltage must be fixed up to 0.5%. Element alignment precision of 0.5 mm are needed.

The quadrupole gradients along the line must be optimized depending on the optical functions at the capture section exit, which will be measured using the spectrometer line. Errors in the measurements of even 50% in the initial optical functions have been simulated and tracked with PARMELA resulting in an emittance degradation of the same order as in the case with no errors, a little more significant in the horizontal plane; the degradation of course is higher for lower initial emittances. The beam envelopes are perturbed but not in a significant way; the final betatron functions can still be matched to the SC Linac transport. The final bunch length is almost independent on the initial transverse conditions: only differences of some tenths of millimetres have been observed.

Errors of the order of 1% in the initial energy measurements have been also simulated and they do not affect much the final bunch length nor the transverse behaviour.

Distortions in the nominal trajectory caused by magnet misalignments in the line have been studied with the code DIMAD⁹.

In each quadrupole along the line there will be installed a monitor and a corrector as an additional winding which can be used in the two transverse planes¹⁰. The optimum correction scheme is based on the 'local correction': 10 correctors, of which 6 are for the vertical correction in the defocusing quadrupoles and 4 for the horizontal correction in the focusing quadrupoles. A steering used as an additional corrector will give the final kick to the orbit as close as possible to the linac entrance.

The correction has been simulated for rms values of the misalignment gaussian distribution $\sigma_{x,y}=0.5$ mm, $\sigma_{\theta,\phi}=0.5$ mrad. The rms value of the orbit is decreased by a factor ~ 10 (or even 20 in the vertical plane) if the initial beam coordinates are zero, while only a factor $\sim 3/4$ is obtained if the beam is not aligned at the input of the line as can be expected because the errors of the quadrupoles can be corrected directly with the correcting windings, while an initial perturbation cannot be eliminated, but just propagated along the line.

References

- [1] F. Tazzioli et al.: "Status of the LISA Superconducting Linac Project", these Proceedings.
- [2] A. Aragona, C. Biscari, R. Boni, S. Kulinski, B. Spataro, F. Tazzioli, M. Vescovi, "Injector for LISA", Proceedings of the 1988 Linear Accelerator Conference - CEBAF 1988, p.400.
- [3] R. Boni, A. Gallo, F. Tazzioli: "The RF System of the Frascati LISA 1 MeV Injector", these Proceedings.
- [4] S. Kulinski, M. Vescovi: "A Gun for LISA", Internal Report LNF-87/98(R).
- [5] J. Bigolas et al.: "Design and Construction of 1MeV S.W. Accelerator Structure for LISA", these Proceedings.
- [6] C. Biscari, R. Boni, M. Castellano, A. Gallo, B. Spataro: "Bunch length measurement system in the injector section of the SC Linac LISA", Internal Report LNF 90/024 (1990).
- [7] K. Crandall et al.: "Program PARMELA", Los Alamos National Laboratory.
- [8] S. Kulinski: "Semianalytical formulas for extended fringing LIS-73, 1990.
- [9] R.V. Servranckx, K.L. Brown, D. Douglas: "User guide to the program DIMAD", SLAC report 285 UC-28 (A) - 1985
- [10] N. Cavallo et al.: "LISA control system", these Proceedings.